Since January 2020 Elsevier has created a COVID-19 resource centre with free information in English and Mandarin on the novel coronavirus COVID-19. The COVID-19 resource centre is hosted on Elsevier Connect, the company's public news and information website.

Antiviral Research 196 (2021) 105209

Contents lists available at ScienceDirect

Antiviral Research

journal homepage: www.elsevier.com/locate/antiviral

2-((1H-indol-3-yl)thio)-N-phenyl-acetamides: SARS-CoV-2 RNA-dependent RNA polymerase inhibitors

Jianyuan Zhao [a,1], Guoning Zhang [a,1], Yongxin Zhang [a,1], Dongrong Yi [a], Quanjie Li [a], Ling Ma [a], SaiSai Guo [a], Xiaoyu Li [a], Fei Guo [b], Rongtuan Lin [c], Gia Luu [c], Zhenlong Liu [c,*], Yucheng Wang [a,**], Shan Cen [a,***]

[a] Institute of Medicinal Biotechnology, Chinese Academy of Medical Science, Beijing, China
[b] Institute of Pathogen Biology, Chinese Academy of Medical Science, Beijing, China
[c] Lady Davis Institute for Medical Research, McGill University and Jewish General Hospital, Montreal, Quebec, Canada

ARTICLE INFO

Keywords:
COVID-19
SARS-CoV-2
RdRp
Nucleotide analog inhibitor
Remdesivir
2-((1H-indol-3-yl)thio)-N-Phenyl-acetamides

ABSTRACT

Severe acute respiratory syndrome coronavirus-2 (SARS-CoV-2) is the causative agent of Coronavirus Disease 2019 (COVID-19) pandemic. Despite intensive and global efforts to discover and develop novel antiviral therapies, only Remdesivir has been approved as a treatment for COVID-19. Therefore, effective antiviral therapeutics are still urgently needed to combat and halt the pandemic. Viral RNA-dependent RNA polymerase (RdRp) of SARS-CoV-2 demonstrates high potential as a reliable target for the development of antivirals. We previously developed a cell-based assay to assess the efficiency of compounds that target SARS-CoV-2 RdRp, as well as their tolerance to viral exoribonuclease-mediated proof-reading. In our previous study, we discovered that 2-((1H-indol-3-yl)thio)-N-phenyl-acetamides specifically targets the RdRp of both respiratory syncytial virus (RSV) and influenza A virus. Thus, we hypothesize that 2-((1H-indol-3-yl)thio)-N-phenyl-acetamides may also have the ability to inhibit SARS-CoV-2 replication by targeting its RdRp activity. In this research, we test a compound library containing 103 of 2-((1H-indol-3-yl)thio)-N-phenyl-acetamides against SARS-CoV-2 RdRp, using our cell-based assay. Among these compounds, the top five candidates strongly inhibit SARS-CoV-2 RdRp activity while exhibiting low cytotoxicity and resistance to viral exoribonuclease. Compound 6-72-2a is the most promising candidate with the lowest EC_{50} value of 1.41 μM and highest selectivity index (CC_{50}/EC_{50}) (above 70.92). Furthermore, our data suggests that 4–46b and 6-72-2a also inhibit the replication of HCoV-OC43 and HCoV-NL63 virus in a dose-dependent manner. Compounds 4–46b and 6-72-2a exhibit EC_{50} values of 1.13 μM and 0.94 μM, respectively, on HCoV-OC43 viral replication. However, higher concentrations of these compounds are needed to effectively block HCoV-NL63 replication. Together, our findings successfully identified 4–46b and 6-72-2a as promising inhibitors against SARS-CoV-2 RdRp.

1. Introduction

The coronavirus disease 2019 (COVID-19) pandemic, caused by severe acute respiratory syndrome coronavirus 2 (SARS-CoV-2) continues to ravage the globe. As a highly prevalent threat to public health, it is responsible for more than 247.3 millions infections and 5 million deaths worldwide (JHU, 2020). Despite enormous vaccination campaigns across many continents, the lack of effective treatments and therapeutics contribute to massive global increases in the number of infections daily (JHU, 2020; Beigel et al., 2020). In addition to the recently discovered SARS-CoV-2, six other human coronaviruses (HCoVs) have been previously identified: HCoV-229E, HCoV-OC43, HCoV-NL63, HCoV-HKU1, severe acute respiratory syndrome coronavirus (SARS-CoV) and Middle East respiratory syndrome coronavirus (MERS-CoV). HCoV-229E, HCoV-OC43, HCoV-NL63, HCoV-HKU1 associate with mild symptoms and account for 15%–30% cases of common colds (Malik, 2020). These

* Corresponding author.
** Corresponding author.
*** Corresponding author.
E-mail addresses: zhenlong.liu@mail.mcgill.ca (Z. Liu), wangyucheng@imb.pumc.edu.cn (Y. Wang), shancen@imb.pumc.edu.cn (S. Cen).
[1] These authors have contributed equally to this work and share first authorship.

https://doi.org/10.1016/j.antiviral.2021.105209
Received 16 July 2021; Received in revised form 3 November 2021; Accepted 15 November 2021
Available online 18 November 2021

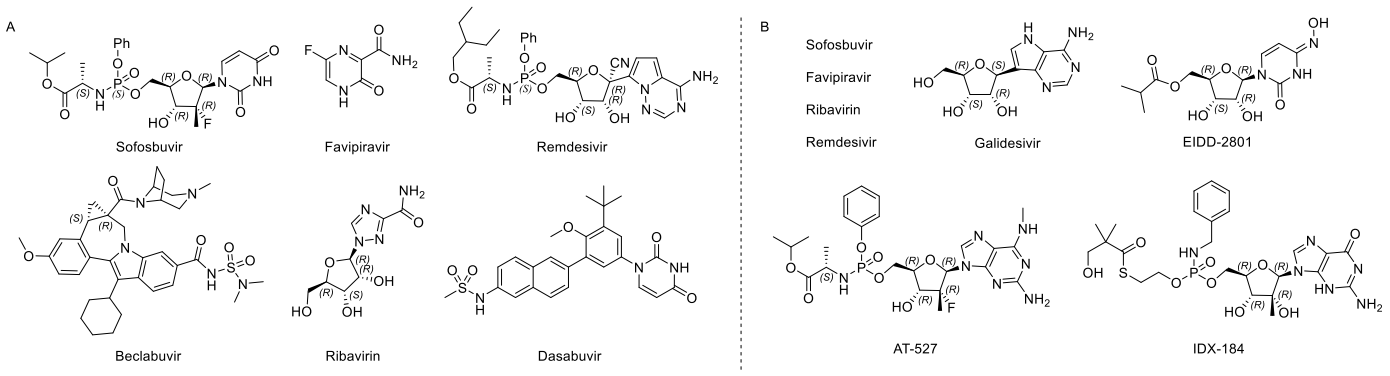

Fig. 1. (A) Structures of FDA-approved antiviral agents targeting RdRp and (B) RdRp inhibitors repurposing for the COVID-19 pandemic.

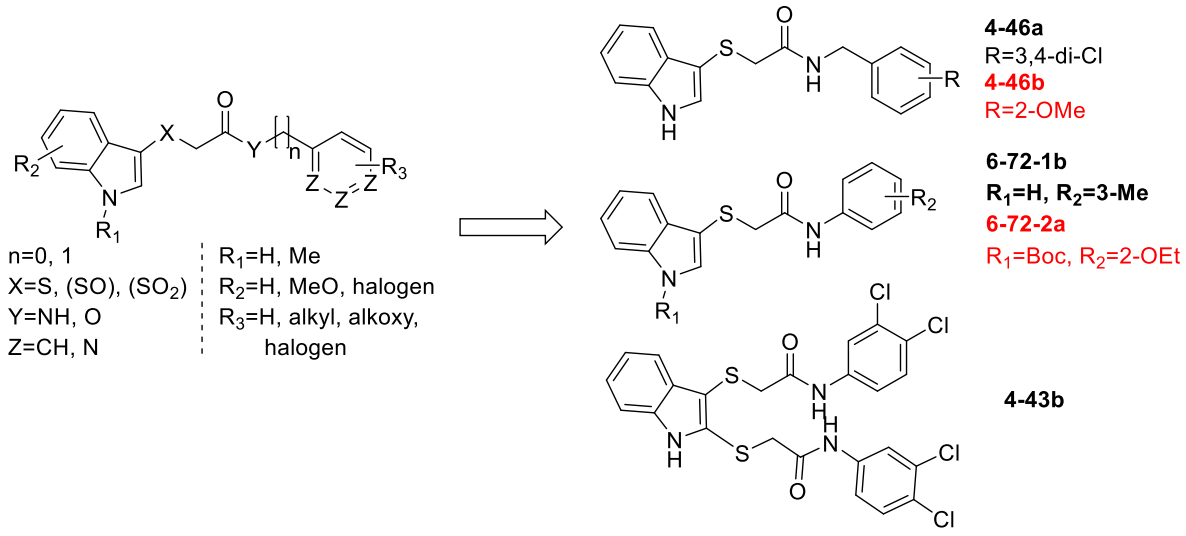

Fig. 2. The main compound skeletons in our RdRp targeting library and anti-SARS-CoV-2 candidates discovered.

four HCoVs are often used as tools for viral pathogenic studies and drug developments, most notably for the current COVID-19 pandemic. Particularly, the RdRp sequences are highly conserved across different CoVs, this is especially true for SARS-CoV-2 and HCoV-OC43 which belong in the same genus beta-coronavirus. Although several therapeutic agents such as Remdesivir have been approved as treatments by the FDA, no antiviral therapies so far have compelling evidence to be effective and the development of new antiviral agents remains imperative.

The SARS-CoV-2 genome ranges from 29.8 kb to 29.9 kb, and contains two open reading frames 1 (Orf1): Orf1a and Orf1b. Orf1b encodes 16 non-structural proteins (nsp1 to nsp16). Among them, the papain-like protease (nsp3), chymotrypsin-like main protease (3CL protease, nsp5), primase complex (nsp7–nsp8), RNA-dependent RNA polymerase RdRp (nsp12), helicase (nsp13), and exoribonuclease (nsp14) are crucial for SARS-CoV-2 replication (Zhu et al., 2020; Jiang et al., 2021; Shannon et al., 2020; Shuhui Song et al., 2020). As previously addressed, RdRp is one of the most promising targets for the development of anti-SARS-CoV-2 therapeutics. Aside from playing a crucial role in viral RNA synthesis, RdRp lacks cellular homologues and is highly conserved in terms of sequence and structure among coronaviruses (Chien, 2020; Hillen, 2020; Aftab et al., 2020; Shyr et al., 2020; Zhao et al., 2021a). As previously shown, RdRp complex is comprised of catalytic subunit nsp12, two accessory subunits nsp7 and nsp8, and RNA template-product duplex(Hillen, 2020; Gao et al., 2020). Nucleos(t)ide analogues (NAs) are potent RdRp inhibitors and restrict viral replication by incorporating into the nascent viral RNA, inducing the termination or reduction of RNA synthesis (Zhu et al., 2020; Shannon et al., 2020). However, the SARS-CoV-2 nsp14 exoribonuclease contributes to resistance of RdRp to NAs by excising erroneous nucleotides incorporated by nsp12 into viral RNA (Smith et al., 2013). Thus, it is necessary to incorporate nsp14 in the screening system for RdRp inhibitors. An additional complication when using NAs is that these compounds must be metabolized to become 5′-triphosphate molecules after entering the host cell to be active (Shannon et al., 2020; Jockusch et al., 2020; Wang et al., 2020). To avoid the complex and time-consuming synthesis process of nucleoside triphosphate, we have built a cell-based assay using Gaussia-luciferase (Gluc) reporter to directly assess the capacity of NAs targeting SARS-CoV-2 RdRp without synthesizing the active nucleoside triphosphate form (Zhao et al., 2021a).

Currently, six RdRp inhibitors have been approved to use as antiviral drugs that includes 3 nucleos(t)ide analogues, Sofosbuvir, Remdesivir and Ribavirin; 1 nucleobase analog, *Favipiravir* and 2 nonnucleos(t)ide analogues, Beclabuvir (in combination with Asunaprevir and Daclatasvir) and Dasabuvir (in combination with ombitasvir/paritaprevir/ritonavir) (Fig. 1A). In addition, other potential RdRp inhibitors exist, and these have been comprehensively summarized by Tian et al. (2021). Many RdRp inhibitors have been repurposed for the COVID-19 pandemic, and at least 8 of them have shown significant anti-SARS-CoV-2 activity at the cellular level or in clinical trials (Fig. 1B).

Our previous study has demonstrated that 2-((1H-indol-3-yl)thio)-N-phenyl-acetamides target specifically RdRp of both respiratory syncytial virus (RSV) and influenza A virus, resulting into inhibition of viral

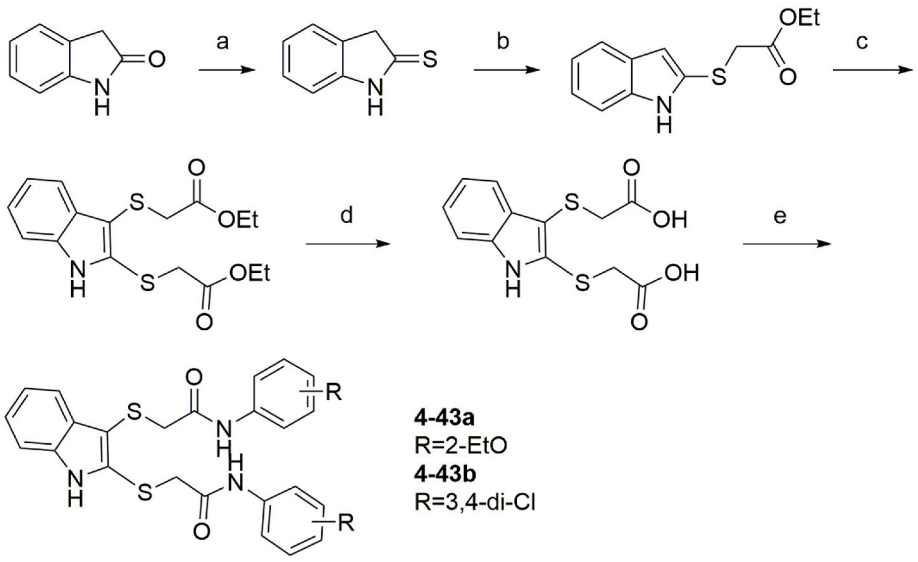

Scheme 1. Synthetic scheme for compounds 4–43a and 4–43b. Reagents and conditions: **(a)** P_2S_5, THF, reflux;**(b)** Ethyl 2-bromoacetate, potassium Carbonate, DMF; **(c)** Sodium S-(2-ethoxy-2-oxoethyl) sulfurothioate, Iodine, DMSO, 60 °C; **(d)** NaOH, EtOH/H_2O; **(e)** Substituted aniline, HATU, DIEA, dichloromethane.

replication at sub-micromolar EC_{50} values with lower cytotoxicity comparing with ribavirin (Zhang et al., 2020). We hypothesize that the 2-((1H-indol-3-yl)thio)-N-phenyl-acetamides could also inhibit SARS-CoV-2 through targeting its RdRp. Thus, a small-scale compound library containing mainly 2-((1H-indol-3-yl)thio)-N-phenyl-acetamide (Fig. 2) was evaluated for the anti-SARS-CoV-2 activity. Using our cell-based Gluc assay, we identified several anti-SARS-CoV-2 candidates from this library. The five most effective candidates showed a dose-dependent inhibition of SARS-CoV-2 RdRp with EC_{50} values ranging from 1.41 to 3.07 μM. Encouragingly, two of these candidates were efficient SARS-CoV-2 RdRp inhibitors, with activity levels close to Remdesivir. It is worth mentioning that there are only two compounds with a skeleton of 2-((indol-3-yl)thio)-N-**benzyl**-acetamides in the screened library and both of them were in the top 5 effective candidates. Thus, we have reported that a new series of 2-((indol-3-yl)thio)--N-**benzyl**-acetamides was synthesized and evaluated for its SARS-CoV-2 RdRp inhibitory effect and a more potent candidate against HCoV-OC43 than Remdesivir, recently (Zhang et al., 2021).

2. Materials and methods

1. Cells, transfection, and viruses

HEK293T, A549, and LLC-MK2 cells were cultured in Dulbecco's modified Eagle's medium (DMEM; Gibco, Thermo Fisher Scientific, Waltham, MA, USA) with 10% (v/v) fetal bovine serum (FBS; Gibco). HCT-8 cells cultured in RPMI1640 medium with 10% FBS. Plasmids transfections were performed using Vigofect transfection reagents (Vigorous) according to the manufacturer's instructions. HCoV-OC43 (VR-1558) was used to infect HCT-8 cells at an MOI of 0.1. The HCoV-NL63 strain Amsterdam I was used to infect LLC-MK2 cells at an MOI of 0.01.

2. Plasmids, compounds, and reagents

Codon-optimized pCOVID19-nsp12, pCOVID19-nsp7, pCOVID19-nsp8, pCOVID19-nsp10 and pCOVID19-nsp14 expression vectors encoded flag-tagged nsp12, nsp7, nsp8, nsp10 and nsp14 at their C-terminus, respectively. The plasmid pCoV-Gluc expressed the Gaussia-luciferase (Gluc) reporter gene flanked by 5′ and 3′ untranslated regions (UTRs) of SARS-COV-2 under the control of the CMV (cytomegalovirus) promoter. Briefly, 5′UTR-Gluc-3′UTR was first synthesized (Sangon Biotech) and then inserted into the BamHl and Notl sites of pRetroX-tight-Pur vector (kindly provided by Dr. Guo Fei) following amplication with the forward primers were for (5′-GGC GGA TCC ATT AAA GGT TTA TAC-3′) and reverse primed (5′-TTA GCG GCC GCG TCA TTC TCC TAA GAA-3′). Remdesivir (S8932) and Ribavirin (S2504) were obtained from Selleck chemicals (Houston, TX, USA) and dissolved in DMSO. A library of 103 2-((1H-indol-3-yl)thio)-N-phenyl-acetamides derivatives was synthesized and a stock solution (10 mM) was prepared in dimethyl sulfoside (DMSO) (Table S1 in supplemental materials).

3. RNA isolation and Real-time RT-PCR

HEK293T cells were grown in DMEM containing 10% FBS for 24 h before treatment with 5 μM or 10 μM Remdesivir or compounds for 24 h. Total RNA was extracted with Aurum Total RNA mini kit. cDNA was synthesized using primer plus-Gluc-RT (5′-TGG ATC TTG CTG GCG AAT GT-3′) or minus-Gluc-RT (5′-ACT GTC GTT GAC AGG ACA CG-3') for 1 h at 37 °C. The cDNAs were quantified using Applied Biosystems QuantStudio (Thermo Fisher Scientific). Expression levels were normalized with GAPDH level. Primers Gluc Forward (5′-CGG GTG TGA CCG AAA GGT AA-3′) and Reverse (5′-TGG ATC TTG CTG GCG AAT GT-3′) were applied for PCR. GAPDH primers were Forward (5′-GTC CAC TGG CGT CTT CAC CA-3′) and reverse (5′-GTG GCA GTG ATG GCA TGG AC-3′).

4. Cell toxicity assay

Cell toxicity was measured in the water-soluble tetrazolium salt-8 (WST-8) reagent (CCK-8, Beyotime). Each compound was added to HEK293T cells at concentration ranging from 0.78 to 100 μM for 24-h incubation. Then, 10 μL CCk-8 was added to each well for 1h incubation at 37 °C. The absorbance at 450 nm was measured using the Enspire 2300 Multiable reader (PekinElmer). The 50% cytotoxic concentration (CC_{50}) was analyzed by comparing the viability of test compounds-treated cells and DMSO-treated cells.

5. Gluc activity assay

A stock of coelenterazine-h (Promega, Madison, WI, USA) was dissolved in absolute ethyl alcohol to a concentration of 1.022 mmol/L. Briefly, the stock was diluted in PBS to 16.7 μM and incubated in the dark for 30 min at room temperature. For the luminescence assay, 10 μL of culture medium was added to each well of a 96-well plate and mixed

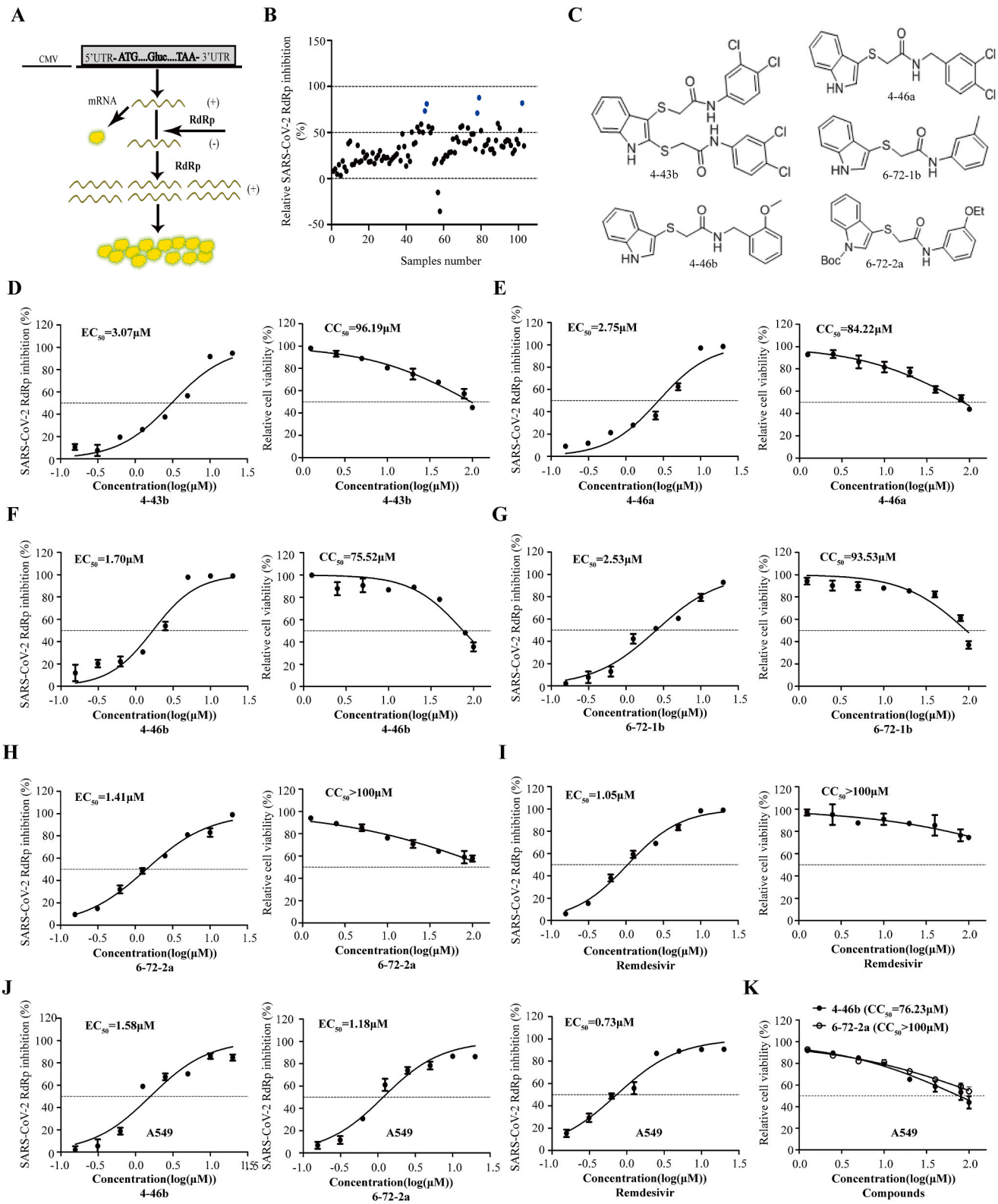

Fig. 3. Inhibition of SARS-CoV-2 RdRp by 2-((1H-indol-3-yl)thio)-N-phenyl-acetamides. (A) Schematic of the CoV-RdRp-Gluc reporter assay. (B) Overview of the results from the CoV-RdRp-Gluc reporter assay. (C) Chemical structure of top five compounds. (D–I) Dose-response curves (EC_{50}/CC_{50}) for top five compounds. HEK293T cells were transfected with CoV-Gluc, nsp12, nsp7, and nsp8 expression vector at a ratio of 1:10:30:30. Twelve hours post transfection, cells were re-seeded in 96-well plates (10^4/well) and treated with serially dilution of compounds 4–43b (D), 4-46a (E), 4–46b (F), 6-72-1b (G), 6-72-2a (H) and Remdesivir (I). Gluc activity was measured in harvested medium after 24 h incubation. CC_{50} values were measured in HEK293T cells with CCK-8 kits. (J) The EC_{50} of active compounds against SARS-CoV-2 RdRp in A549 cells. A549 cells (5×10^5) were co-transfected with the indicated plasmids (50 ng, 200 ng, 600 ng and 600 ng for pCoV-Gluc, nsp12, nsp7 and nsp8, respectively). Twelve hours post transfection, cells were re-seeded in 96-well plates (10^4/well) and treated with serially dilution of compounds indicated above. Gluc activity was measured after 72 h incubation. (k) CC_{50} values of the active compounds were measured in A549 cells with CCK-8 kits. (D–K) Results shown are the average of three independent experiments. Error bars indicate SD.

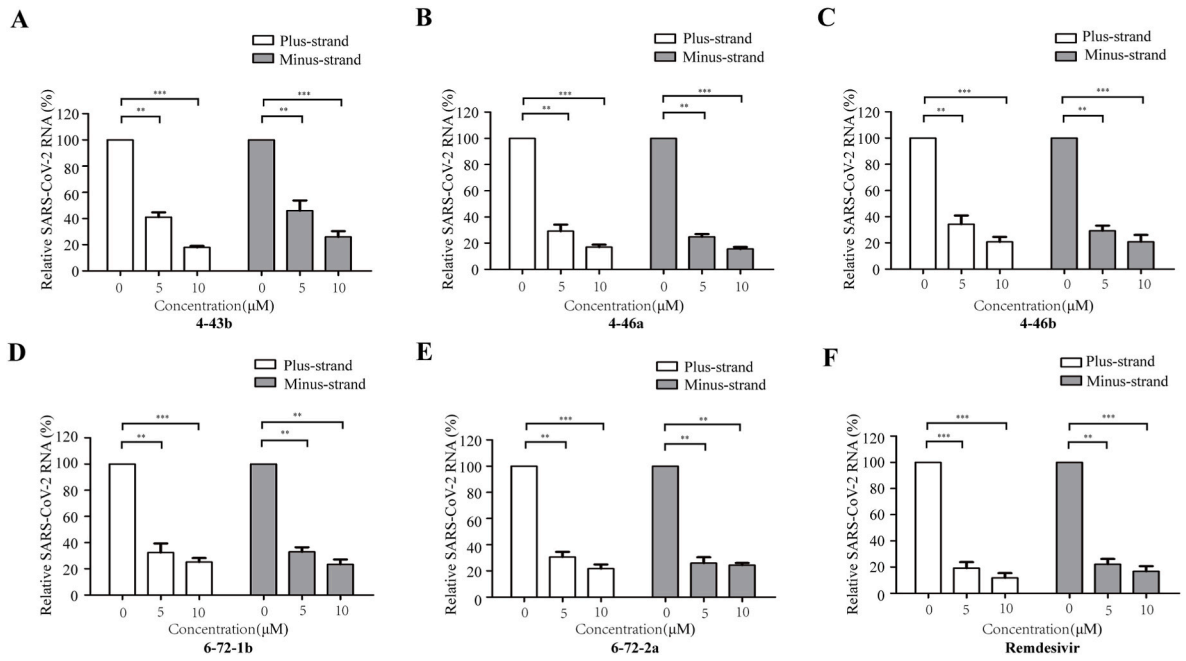

Fig. 4. Reduction of CoV-Gluc RNA synthesis by top five candidates. HEK293T cells were transfected with CoV-Gluc, nsp12, nsp7, nsp8 expression vectors at the ration of 1:10:30:30. Six hours after transfection, cells were replenished with fresh medium containing 4–43b (A), 4-46a (B), 4–46b (C), 6-72-1b (D), 6-72-2a (E), and Remdesivir (F) at 5 μM and 10 μM. After 24 h incubation, total cellular RNA was extracted, and levels of CoV-Gluc RNA were determined by qRT-PCR. Results shown are the average of three independent experiments. Error bars indicate SD. $^{**}P < 0.01$, $^{***}p < 0.001$.

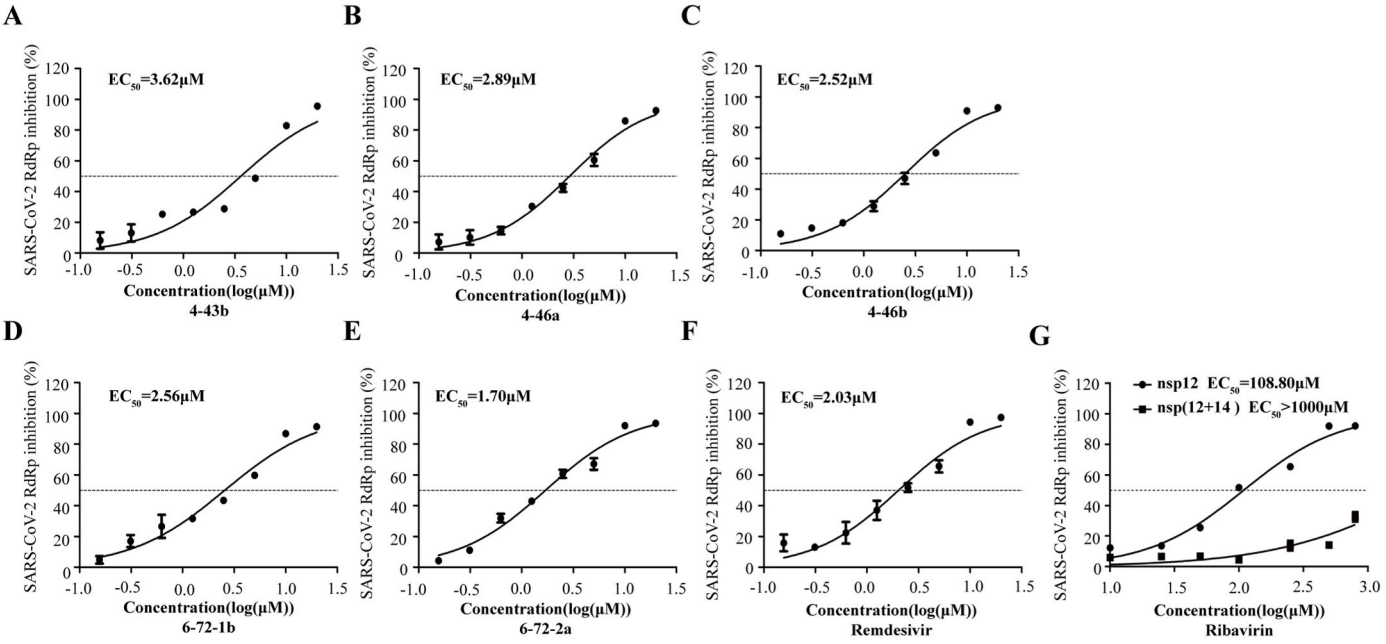

Fig. 5. The top five compounds were resistant to SARS-CoV-2 exoribonuclease. HEK293T cells were transfected with CoV-Gluc, nsp12, nsp7, nsp8, nsp10 and nsp14 plasmid DNA at the ratio of 1:10:30:30:25:25. Twelve hours post transfection, cells were re-seeded in 96-well plates (10^4/well) and treated with serially diluted compounds 4–43b (A), 4-46a (B), 4–46b (C), 6-72-1b (D), 6-72-2a (E), Remdesivir (F) and Ribavirin (G). After 24 h, Gluc activity in supernatants were quantified. Results shown are the average of three independent experiments. Error bars indicate SD.

with 60 μL of 16.7 μM coelenterazine-h. Luminescence was measured during 0.5s using the Berthold Centro XS3 LB 960 microplate luminometer.

6. HCoV-OC43 and HCoV-NL63 cytopathic effects (CPE) assay

The anti-HCoV-OC43 and HCoV-NL63 activity was measured by the MTS Cell Proliferation Colorimetric assay kits (Promega, Madison, WI, USA). Briefly, HCT-8 cells and LLC-MK2 cells were infected with HCoV-OC43 (MOI = 0.1) and HCoV-NL63 (MOI = 0.01) respectively, with 2% FBS and each tested compound. Cells were than incubated at 33 °C for 120 h in 5% CO_2 incubator. Subsequently, 20 μL of MTS Cell Proliferation Colorimetric reagent was added into each well and cells were incubated for 3 h at 37 °C in the presence of 5% CO_2. Cell proliferation

Table 1
Summary of top five compounds toward SARS-CoV-2 RdRp and anti- Coronavirus activity.

Compound	HEK293T					A549		Anti-HCoV-OC43 (EC_{50}/μM)	Anti-HCoV-NL63 (EC_{50}/μM)
	Nsp12 (EC_{50}/μM)	CC_{50}/μM	TI(CC_{50}/EC_{50})	Nsp12 + 14 (EC_{50}/μM)	Ratio (12 + 14/12)	Nsp12 (EC_{50}/μM)	CC_{50}/μM		
4–43b	3.07	96.19	31.33	3.62	1.18				
4-46a	2.75	84.22	30.63	2.89	1.05				
4–46b	1.70	75.52	44.42	2.52	1.48	1.58	76.23	1.13	>50
6-72-b1	2.53	93.53	36.97	2.56	1.01				
6-72-2a	1.41	>100	>70.92	1.70	1.21	1.18	>100	0.94	12.5
Remdesivir	1.05	>100	>95.24	2.03	1.93	0.73		0.82	2.89
Ribavirin	108.8			>1000	>9.18				
4–46b & Remdesivir								0.69	2.13
6-72-2a & Remdesivir								0.60	1.68

was measured at an absorbance at 490 nm using the Enspire 2300 Multiable reader (PekinElmer). HCT-8 cells or LLC-MK2 cells with virus infection but without drugs were used as negative controls to indicate 0% CPE inhibition. The percentage CPE inhibition is shown in the Equation: The percentage CPE inhibition=(A_{490} of samples $-A_{490}$ of negative control)/(A_{490} of positive control $-A_{490}$ of negative control) × 100.

7. Statistical analysis

Data are presented as the means ± SD from at least three independent experiments and the two-tailed *t*-test was used for statistical analysis. Differences between groups were considered statistically significant if $p < 0.01$(**), $p < 0.001$(***).

8. Synthesis

The 2-((1H-indol-3-yl)thio)-N-phenyl-acetamide and 2-((indol-3-yl) thio)-N-benzyl-acetamides were synthesized according to the process we reported early (Zhang et al., 2021). The 2,3-dithioindole were synthesized according to the scheme below (Scheme 1). The 2-indolinone was substituted with phosphorus pentasulfide to introduce the first sulfur atom. The second sulfur atom at the 3-position was introduced by the substitution reaction of the indole ring by the Bunte salt. The diacid obtained by hydrolysis is coupled with the substituted aniline to obtain the product 4-43a and 4–43b, respectively.

3. Results

1. Screening 2-((1H-indol-3-yl)thio)-N-phenyl-acetamides through the CoV-RdRp-Gluc reporter assay

In our previous study, we have developed a SARS-CoV-2 RdRp-dependent Gluc reporter system (CoV-RdRp-Gluc). It is a cell-based high-throughput screening assay for SARS-CoV-2 RdRp inhibitors based on the measurement of Gluc in culture medium. Briefly, the assay is based on a CMV promoter-driven reporter vector (CoV-Gluc) expressing the Gaussia-luciferase reporter gene flanked by 5′ and 3' untranslated regions (UTRs) of SARS-CoV-2. Gluc RNA is subsequently amplified by SARS-CoV-2 RdRp (nsp12) in the presence of nsp7 and nsp8. Gluc activity thus correlates with the activity of SARS-CoV-2 RdRp (Fig. 3A) (Zhao et al., 2021a). The CoV-Gluc reporter vector and expression vectors of nsp12, nsp7 and nsp8 were transfected in HEK293T cells, which were exposed to various candidates 12 h post transfection. After 24 h incubation, Gluc activities were measured to evaluate the inhibitory potential of candidates toward SARS-CoV-2 RdRp. Initially, 103 2-((1H-indol-3-yl)thio)-N-phenyl-acetamide candidates were screened through our CoV-RdRp-Gluc reporter assay. As shown in Supplementary Table S1, all 2-((1H-indol-3-yl) thio)-N-acetamides (R1 = R2 = H) showed a inhibition toward RdRp activity except for 4-53c and 4-53d. 2-((1H-indol-3-yl)thio)--N-(bromophenyl)acetamide (R3 = bromoaniline) (1-HB-9 and 1-HB-10) showed the strongest inhibitory potential in the acetanilide. When aniline was substituted with benzylamine in R3, their inhibitory activity was significantly enhanced (4–46b, 4–48 vs. 1-HB-3, 1-HB-5). After the introduction of a methoxy group, a chlorine atom or a 5- bromine atom to the benzene ring in indole, a 2–15 folds increase in inhibitory potential was observed. A methyl- or a tert-butoxycarbonyl- substitution in R2 was also beneficial to the inhibitory activity. When sulfide was oxidized to sulfoxide or sulfone, no significant changes in RdRp inhibition was noted. When a similar substitution was introduced to the 2, 3-position on indole, RdRp inhibition was improved in comparison to compounds with a single 3-position substitution (4-43a and 4–43b). Importantly, 19 candidates repressed SARS-CoV-2 RdRp activity more than 50% at a 10 μM concentration and the top five of them shown as blue spot in Fig. 3B can markedly repress SARS-CoV-2 RdRp activity at around 80% at 10 μM ($P < 0.005$). Among them, 6-72-2a surprisingly showed similar inhibition effect as Remdesivir (Table S1). The lipophilic Boc-group may contribute to the activity and a similar result was discovered in our another research, in which the stability of the Boc-group was also demonstrated (Zhao et al., 2021b). The structures of these five compounds also suggest that chemical structure of 2-((1H-indol-3-yl)thio) acetamide is pivotal element for its capability against RdRp (Fig. 3C).

2. Evaluation of anti-SARS-CoV-2 RdRp activity of top five compounds

To evaluate the inhibition of the five most effective candidates against SARS-CoV-2 RdRp, EC_{50} and CC_{50} were evaluated for each compound with increasing doses. All top five compounds showed a dose-dependent inhibition of SARS-CoV-2 RdRp activity (Fig. 3D–I). Compound 6-72-2a represented the most promising compound showing the lowest EC_{50} value (1.41 μM) with the highest selectivity index (CC_{50}/EC_{50}) (above 70.92) (Fig. 3H). Compound 4–46b also showed a strong SARS-CoV-2 RdRp inhibition effect with an EC_{50} value of 1.70 μM and CC_{50} value of 75.52 μM (Fig. 3F). EC_{50} values of other tested compounds 4–43b, 4-46a, and 6-72-1b were 3.07 μM, 2.75 μM and 2.53 μM, respectively (Fig. 3D, E, and 3G). Next, we evaluated the inhibition of 4–46b and 6-72-2a with the cell-based assay in A549 cell line. Surprisingly, SARS-CoV-2 RdRp activity was restrained by 4–46b and 6-72-2a, presenting low EC_{50} value of 1.58 μM and 1.18 μM, respectively, which is close to the EC_{50} of Remdesivir 0.73 μM (Fig. 3J). The CC_{50} values of 4–46b and 6-72-2a in A549 cells were 76.25 μM and above 100 μM respectively, which were much higher than their EC_{50} values (Fig. 3K). Together, these data support that 4–46b and 6-72-2a were determined as promising inhibitors against SARS-CoV-2 RdRp. Moreover, we have measured the effect of the active compounds 4–43b, 4-46a, 4–46b, 6-72-1b and 6-72-2a on the expression of the Gluc reporter plasmid in the

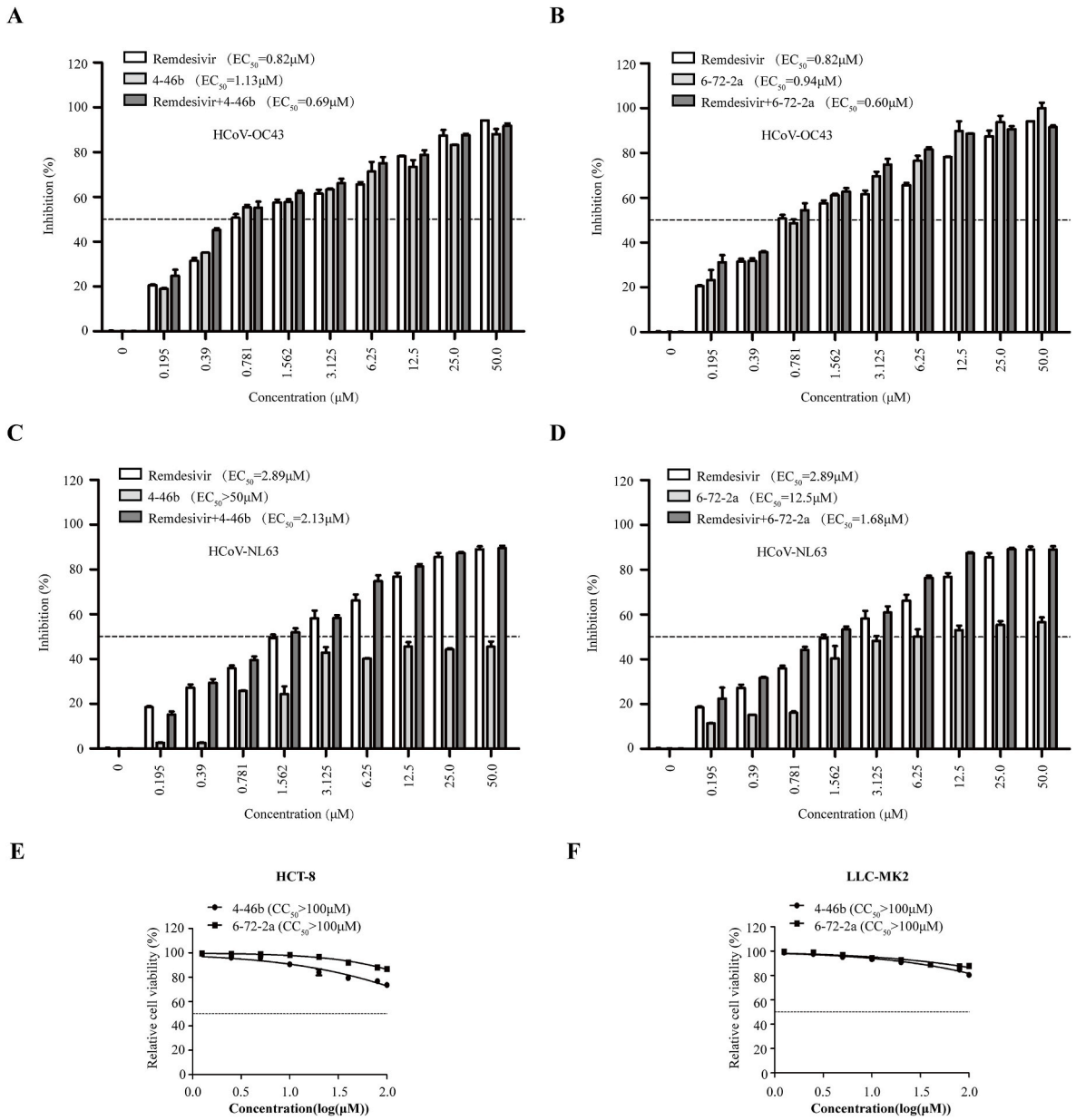

Fig. 6. The anti-HCoV-OC43 and anti-HCoV-NL63 activities of 4–46b and 6-72-2a. HCT-8 and LLC-MK2 cells were seeded in 96-wells for 48h, and then infected with HCoV-OC43 (MOI = 0.1) and HCoV-NL63 (MOI = 0.01) respectively, and subsequently treated with serial dilutions of 4–46b (A and C) or 6-72-2a (B and D) 1-h post-infection. After a 120-h infection, 20 μL of MTS Cell Proliferation Colorimetric reagent was added into each well and cells were incubated for 3 h at 37 °C. Optical density at 490 nm wavelength was measured. (E–F) CC_{50} values of the active compounds were measured in HCT-8 and LLK-MK2 cells with CCK-8 kits. Results shown are the average of three independent experiments. Error bars indicate SD.

absence of viral RdRp. Briefly, HEK293T cells were co-transfected with a pCoV-Gluc plasmid and incubated with the active compounds indicated above, respectively. Then levels of Gluc were determined. The results shown that these compounds have no significant impact on the expression of Gluc in the absence of SARS-CoV-2 RdRp even at a higher concentration of 10 μM (Fig. S1). This suggests that these compounds target the replication of RNA driven by viral RdRp.

3. Reducing the RNA synthesis efficiency of SARS-CoV-2 RdRp by top five compounds

To further confirm the inhibition activity of the selected compounds against SARS-CoV-2 RdRp, RNA synthesis mediated by SARS-CoV-2 RdRp was examined by quantification of the levels of plus-strand and minus-strand RNA of Gluc following treatment with 5 μM and 10 μM of each compound. Compounds diminished the levels of both plus-strand and minus-strand Gluc RNA in a dose-dependent manner (Fig. 4A–E). Compound 6-72-2a reduced both plus-strand and minus-strand RNA levels of controls about 80% at 10 μM, an efficiency comparable to that of our positive control, Remdesivir (Fig. 4F).

4. The tolerance of top five compounds to SARS-CoV-2 exoribonuclease activity

The exoribonuclease nsp14 and its activator nsp10 play an important proofreading function as SARS-CoV-2 replicates. This contributes SARS-CoV-2 RdRp resistant to NA inhibitors, such as ribavirin (Ma et al., 2015; Ferron et al., 2018). Thus, the inhibitory potential of selected compounds was evaluated in the presence of nsp14/nsp10. The CoV-Gluc report vector and the expression vectors of nsp12, nsp7, nsp8, nsp10

and nsp14 were transfected in HEK293T cells, followed by treatment with different dilution of the compounds. As we previously demonstrated, nsp14/nsp10 lead to the inappreciable decrease of Gluc activity (Zhao et al., 2021a). Our results illustrated that all compounds, i.e. 4-43b, 4-46a, 4–46b, 6-72-1b and 6-72-2a showed strong tolerance to the presence of nps14/nsp10 with EC_{50} value of 3.62 μM, 2.89 μM, 2.52 μM, 2.56 μM, 1.70 μM, respectively (Fig. 5A–E). In fact, all compounds presented an inhibitory potential very similar to the activity observed against nsp12 only (ratio 12 + 14/12 were all close to 1). Results obtained with Remdesivir, showed resistance to proofreading activity (EC_{50} value of 2.03 μM; ratio 12 + 14/12 of 1.93) (Fig. 5F and Table 1). However, the nps14/nsp10 markedly increased the EC_{50} value of compound Ribavirin (the ratio 12 + 14/12 is above 9.18) (Fig. 5G and Table 1). Together, these five compounds were identified as specific SARS-CoV-2 RdRp inhibitors, among them, 4–46b and 6-72-2a present the strongest inhibition activity against SARS-CoV-2 RdRp.

5. Assessment of anti-HCoVs activity of compounds 4–46b and 6-72-2a

As HCoV-OC43 and HCoV-NL63 are human coronaviruses are commonly used in preclinical antiviral drug development. Besides, the RdRp sequences are highly conserved across different CoVs and both SARS CoV-2 and HCoV-OC43 are betacoronavirus. Herein, in this cell-based assay, both HCT-8 and LLC-MK2 cell lines were infected with HCoV-OC43 and HCoV-NL63 respectively, followed by measuring the CoV-induced cytopathic effect (CPE) inhibition as an out-put (Li, 2021). Briefly, HCT-8 or LLC-MK2 cells were pretreated with serial dilution of 4–46b and 6-72-2a for 1h, and subsequently infected with HCoV-OC43 and HCoV-NL63, respectively (Fig. 6). Additionally, we also measured the CC_{50} of the compounds 4–46b and 6-72-2a in HCT-8 and LLC-Mk2 cells. The results showed that the CC_{50} values of 4–46b and 6-72-2a were higher than the highest concentrations of the HCoV-OC43 and HCoV-NL63 cytopathic effects (CPE) assay both in HCT-8 and LLC-MK2 cells (Fig. 6E–F). Results demonstrated that both compounds 4–46b and 6-72-2a effectively inhibited HCoV-OC43 and HCoV-NL63 replication in a dose-dependent manner. HCoV-OC43 viral replication demonstrated EC_{50} values of 1.13 μM and 0.94 μM for compounds 4–46b and 6-72-2a, while higher concentrations of these compounds were needed to effectively block HCoV-NL63 replication. However, the EC_{50} values for HCoV-OC43 by the combining of active compounds 4–46b and 6-72-2a with Remdesivir are 0.69 μM and 0.60 μM, respectively; for HCoV-NL63 by combining of 4–46b and 6-72-2a with Remdesivir are 2.13 μM and 1.68 μM, respectively. This suggests that EC_{50} values for HCoV-OC43 and HCoV-NL63 can be reduced by combining these agents with Remdesivir to achieve synergy.

4. Conclusion

To contribute to the ongoing COVID-19 pandemic, intensive efforts in the development of antiviral drugs are still needed. Viral RdRp is one of most valuable targets against SARS-CoV-2. As our previously reported, we developed a CoV-RdRp-Gluc reporter assay and demonstrated that 2-((1H-indol-3-yl)thio)-N-phenyl-acetamides could inhibit RSV and IAV RdRp activity. In this study, we tested 103 2-((1H-indol-3-yl)thio)-N-phenyl-acetamide candidates using an adapted CoV-RdRp-Gluc reporter assay. Five of these compounds effectively inhibited SARS-CoV-2 RdRp and two of them were most effective inhibitors of HCoV-OC43 and HCoV-NL63 replication.

Author contribution

SC, YW and ZL conceived the idea of project. JZ, GZ and YZ performed the experiments. DY and QL helped with the resources. LM and SG contributed to validation. ZL drafted the manuscript. XL, FG, RL, GL and SC reviewed and edited the manuscript. All the authors have read and approved the manuscript for submission.

Notes

The authors declare no competing financial interest.

Declaration of interest statement

We declare that there is no conflict of interest regarding this submission.

Acknowledgments

We appreciate the support of following funds: the National Key Research and Development Program of China [2018YFE0107600 and 2016YFD0500307], the National Natural Science Foundation of China (81772205 and 81902076), CAMS Innovation Fund for Medical Sciences [2021-1-I2M-038], and the Fundamental Research Funds for the Central Universities [33320200046]. The National Infrastructure of Microbial Resources [NIMR-2014-3] and CAMS Collection Center of Pathogenic Micro-organisms [CAMS-CCPM-A] also provide valuable reagents.

Appendix A. Supplementary data

Supplementary data to this article can be found online at https://doi.org/10.1016/j.antiviral.2021.105209.

References

Aftab, S.O., et al., 2020. Analysis of SARS-CoV-2 RNA-dependent RNA polymerase as a potential therapeutic drug target using a computational approach. J. Transl. Med. 18 (1), 275.

Beigel, J.H., et al., 2020. Remdesivir for the treatment of covid-19 - final report. N. Engl. J. Med. 383 (19), 1813–1826.

Chien, M., et al., 2020. Nucleotide analogues as inhibitors of SARS-CoV-2 polymerase, a Key drug target for COVID-19. J. Proteome Res. 19 (11), 4690–4697.

Ferron, F., et al., 2018. Structural and molecular basis of mismatch correction and ribavirin excision from coronavirus RNA. Proc. Natl. Acad. Sci. U. S. A. 115 (2), E162–E171.

Gao, Y., et al., 2020. Structure of the RNA-dependent RNA polymerase from COVID-19 virus. Science 368 (6492), 779–782.

JHU, C.f.S.S.a.E.C.a.J.H.U., https://coronavirus.jhu.edu/map.html, 2020.

Hillen, H.S., et al., 2020. Structure of replicating SARS-CoV-2 polymerase. Nature 584, 154–156.

Jiang, Y., Yin, W., Xu, H.E., 2021. RNA-dependent RNA polymerase: structure, mechanism, and drug discovery for COVID-19. Biochem. Biophys. Res. Commun. 538, 47–53.

Jockusch, S., et al., 2020. A library of nucleotide analogues terminate RNA synthesis catalyzed by polymerases of coronaviruses that cause SARS and COVID-19. Antivir. Res. 180, 104857.

Li, Q., et al., 2021. Corilagin inhibits SARS-CoV-2 replication by targeting viral RNA-dependent RNA polymerase. Acta Pharm. Sin. B 11 (6), 1555–1567.

Ma, Y., et al., 2015. Structural basis and functional analysis of the SARS coronavirus nsp14-nsp10 complex. Proc. Natl. Acad. Sci. U. S. A. 112 (30), 9436–9441.

Malik, Y.A., 2020. Properties of coronavirus and SARS-CoV-2. Malays. J. Pathol. 42 (1), 3–11.

Shannon, A., et al., 2020. Remdesivir and SARS-CoV-2: structural requirements at both nsp12 RdRp and nsp14 Exonuclease active-sites. Antivir. Res. 178, 104793.

Shuhui Song, L.M., Dong, Zou, Tian, Dongmei, Li, Cuiping, Zhu, Junwei, Chen, Meili, Wang, Anke, Ma, Yingke, Li, Mengwei, Teng, Xufei, Cui, Ying, Duan, Guangya, Zhang, Mochen, Jin, Tong, Shi, Chengmin, Du, Zhenglin, Zhang, Yadong, Liu, Chuandong, Li, Rujiao, Zeng, Jingyao, Hao, Lili, Jiang, Shuai, Chen, Hua, Han, Dali, Xiao, Jingfa, Zhang, Zhang, Zhao, Wenming, Xue, Yongbiao, Bao, Yiming, 2020. The global landscape of SARS-CoV-2 genomes, variants, and haplotypes in 2019nCoVR. Genomics, Proteomics & Bioinformatics 18 (6), 749–759. https://doi.org/10.1016/j.gpb.2020.09.001.

Shyr, Z.A., et al., 2020. Drug discovery strategies for SARS-CoV-2. J. Pharmacol. Exp. Therapeut. 375 (1), 127–138.

Smith, E.C., et al., 2013. Coronaviruses lacking exoribonuclease activity are susceptible to lethal mutagenesis: evidence for proofreading and potential therapeutics. PLoS Pathog. 9 (8), e1003565.

Tian, L., et al., 2021. RNA-dependent RNA polymerase (RdRp) inhibitors: the current landscape and repurposing for the COVID-19 pandemic. Eur. J. Med. Chem. 213, 113201.

Wang, Q., et al., 2020. Structural basis for RNA replication by the SARS-CoV-2 polymerase. Cell 182 (2), 417–428 e13.

Zhang, G.N., et al., 2020. Design and synthesis of 2-((1H-indol-3-yl)thio)-N-phenyl-acetamides as novel dual inhibitors of respiratory syncytial virus and influenza virus A. Eur. J. Med. Chem. 186, 111861.

Zhang, G.N., et al., 2021. Discovery and optimization of 2-((1H-indol-3-yl)thio)-N-benzyl-acetamides as novel SARS-CoV-2 RdRp inhibitors. Eur. J. Med. Chem. 223, 113622.
Zhao, J., et al., 2021a. A cell-based assay to discover inhibitors of SARS-CoV-2 RNA dependent RNA polymerase. Antivir. Res. 190, 105078.
Zhao, J., et al., 2021b. Quinoline and quinazoline derivatives inhibit viral RNA synthesis by SARS-CoV-2 RdRp. ACS Infect. Dis. 7 (6), 1535–1544.
Zhu, W., et al., 2020. RNA-dependent RNA polymerase as a target for COVID-19 drug discovery. SLAS Discov 25 (10), 1141–1151.